Appeared in: *Computational Methods in Water Resources XIII, Vol. 2*, Bentley et al., eds. 913-920, Balkema, 2000.

An implicit time-marching algorithm for 2-D GWC shallow water models

K.M. Dresback & R.L. Kolar

School of Civil Engineering and Environmental Science, University of Oklahoma, Norman, Oklahoma, USA

ABSTRACT: Currently, wave equation models discretize the generalized wave continuity equation with a three-time-level scheme centered at *k* and the momentum equation with a two-time-level scheme centered at *k*+1/2; nonlinear terms are evaluated explicitly. However in highly nonlinear applications, the algorithm becomes unstable for high Courant numbers. This paper examines the use of an implicit treatment of the nonlinear terms by using an iterative predictor-corrector algorithm. This algorithm was chosen because it is easy to implement in the framework of existing codes and because it minimizes the size of the matrices that must be stored and inverted. Two-dimensional results show over a eight-fold increase in the size of the stable time step, depending on grid resolution and domains. Sensitivity of stability to variations in the *G* parameter was examined; results show that the greatest increase in stability occurred when G/τ_{max} = 1 to 10.

1 INTRODUCTION

Shallow water equations are based on depth-averaged equations of motion, subject to the assumption of a hydrostatic pressure distribution; they are used by researchers and engineers to model the hydrodynamic behavior of oceans, coastal areas, estuaries, lakes and impoundments. Early finite element solutions of the primitive shallow equations were plagued with spurious oscillations. Lynch & Gray (1979) introduced the wave continuity equation (WCE), which suppressed the spurious oscillations without having to dampen the solution either numerically or artificially. Kinnmark (1986) determined that there was no loss in the wave propagation characteristics of the wave continuity equation if, during the formulation, the bottom friction τ is replaced by a numerical parameter *G*, thus developing the generalized wave continuity equation (GWCE). Several models have been developed using this approach since its conception twenty years ago, including the model used in this paper, ADCIRC (an ADvanced 3-D CIRCulation model) (Luettich et al. 1991, Westerink et al. 1992).

Many sources provide the full shallow water equations (Blain 1994, Luettich et al. 1991); for brevity only the GWCE and non-conservative form of the momentum (NCM) equation will be shown. They form the basis of the ADCIRC model. Each equation shown below has abbreviations appearing above the nonlinear terms, which will be discussed in subsequent sections.

GWCE

$$W^G \equiv \frac{\partial^2 \zeta}{\partial t^2} + \overset{\text{“Gg”}}{G\frac{\partial \zeta}{\partial t}} + \overset{\text{“bg”}}{G\nabla\bullet(H\mathbf{v})} - \tau\nabla\bullet(H\mathbf{v}) -$$

$$\overset{\text{“ag”}}{\nabla\bullet\{\nabla\bullet(H\mathbf{v}\mathbf{v})} + H\mathbf{f}\times\mathbf{v} + H\nabla\left[\frac{p_a}{\rho} + g(\zeta - \alpha\eta)\right] - \mathbf{A} +$$

$$\frac{1}{\rho}\nabla\bullet(H\mathbf{T})\} - H\mathbf{v}\bullet\nabla\tau = 0 \qquad (1)$$

NCM Equation

$$\mathbf{M} \equiv \frac{\partial \mathbf{v}}{\partial t} + \overset{\text{“am”}}{\mathbf{v}\bullet\nabla\mathbf{v}} + \overset{\text{“bm”}}{\tau\mathbf{v}} + \mathbf{f}\times\mathbf{v} + \nabla\left[\frac{p_a}{\rho} + g(\zeta - \alpha\eta)\right]$$

$$-\frac{\mathbf{A}}{H} - \frac{1}{\rho H}\nabla\bullet(H\mathbf{T}) = 0 \qquad (2)$$

where ζ is free surface elevation relative to the geiod, *G* is the GWCE numerical parameter, *t* is time, $H = h + \zeta$ is the total water column depth, *h* is the bathymetric depth relative to the geiod, **f** is the Coriolis parameter, p_a is the atmospheric pressure at the free surface, **v** is the depth-averaged velocity, *g* is the acceleration due to gravity, τ represents bottom friction that is parameterized using a Chezy-type empir-

ical relation, ρ is the density of water, α represents the Earth elasticity factor, **T** is the macroscopic stress tensor and η is the Newtonian equilibrium tidal potential (Blain 1994).

A number of early finite element studies looked at time marching, but often from a noise suppression point-of-view. For example, Lee & Froehlich (1986) summarize several time-marching procedures in their review paper on shallow water equations, which covers everything from the trapezoidal rule to three-level semi-implicit schemes. Gray & Lynch (1977) showed several of the same time-marching procedures in greater detail. They indicate that the best scheme for finite element shallow water models is the three-level semi-implicit scheme. Several years later Kinnmark & Gray (1984) examined an alternative semi-implicit wave equation that produced accurate results, yet still treated some nonlinear terms explicitly. However, little recent work with GWCE-based models has been devoted to alternative time-marching algorithms. The intent of this study is to fill the gap, viz, an implicit treatment of nonlinear terms in both the GWCE and momentum equation.

Motivation for this study comes from nonlinear applications having stability problems unless a severe Courant number restriction is imposed. In practice, we have found that a practical upper bound of the Courant number is 0.5 in other to maintain stability; an even tighter constraint must be imposed if the simulation includes barrier islands and constricted inlets. In order to relax this restriction, an alternative time-marching procedure was proposed that treats the dominant nonlinear terms implicitly (Kolar et al. 1998). This paper explores the use of a predictor-corrector algorithm rather than simultaneous integration of the full nonlinear equations since it is easier to implement in the existing framework of ADCIRC. It also minimizes the size of the matrices that must be stored and inverted. We examine the impact of the algorithm on stability and parameter sensitivity in the context of two-dimensional applications.

2 THE TIME-MARCHING ALGORITHM

As a point of departure, let us examine the current time-marching algorithm in ADCIRC. It is a semi-implicit evaluation, i.e., an explicit evaluation of the nonlinear terms with an implicit treatment of the linear terms. For the past and present time levels in ADCIRC, the elevation and velocity values are known due to initial conditions or previous calculations. For the linear terms, the original algorithm uses the elevation and velocity values for the past (*k*-1) and the present (*k*) to calculate the future time level's values. Nonlinear terms are evaluated using only the elevation and velocity values at the present time level (*k*). Kolar et al. (1998) hypothesized that the stability constraint stems primarily from the explicit treatment of the nonlinear terms.

For the nonlinear terms to be evaluated implicitly, a two-stage predictor-corrector time-marching algorithm is introduced. In this case the predictor stage is equivalent to the original algorithm, i.e., it evaluates the nonlinear terms using the values from the present. Estimates of future values obtained from the predictor step (called *k**) and the already known present (*k*) and past (*k*-1) values are then used to obtain the corrected values for the future time level (*k*+1). The corrector stage can be repeated as many times as necessary until convergence.

Both the GWCE and NCM equations contain nonlinear terms. Our study primarily focuses on six dominant nonlinear terms that are identified in (1) and (2). Four of the nonlinear terms appear in the GWCE: advective (abbreviated ag), finite amplitude (abbreviated fg), GWCE flux times *G* (abbreviated Gg) and GWCE flux times τ (abbreviated bg); two appear in the NCM equation: the advective term (abbreviated am) and the bottom friction term (abbreviated bm).

Figure 1 shows the pseudo code for the predictor-corrector algorithm for one of the nonlinear terms. Time weights are introduced that multiply the nonlinear terms at different levels. Choosing the appropriate time weights for the nonlinear terms is an issue in the new algorithm. Note that usage of the time weights only occurs in the corrector step because the nonlinear terms are evaluated explicitly in the predictor step. In Figure 1, the time weights are noted by the abbreviations mentioned earlier with a number following the abbreviation that represents the time level, i.e., 1=time level *k*+1 or *k**, 2=time level *k* and 3=time level *k*-1. The first box contains the predictor

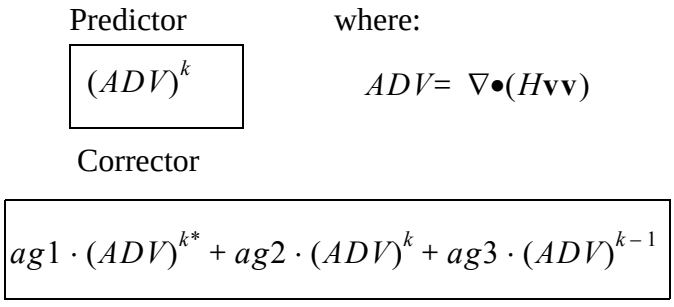

Figure 1. Predictor-Corrector algorithm for the GWCE advective term "ag"

step; it uses no time weights and provides the estimate of the elevation and velocity values at the future time level (*k**). The second box contains the corrector step; it contains time weights that are multiplied by the nonlinear term. The coefficients *ag*1, *ag*2 and *ag*3 are the time weights for the *k*+1 (or *k**), *k*, *k*-1 time levels (future, present and past), respectively, for the advective term of the GWCE. Nomenclature for the other nonlinear terms follows the same pattern. In theory, the time weighting coefficients may equal any value

as long as they sum to one; for practical reasons, the values are restricted to lie between 0 and 1. Examples are shown in Table 1.

Table 1. Possible Combinations of the Time Weighting Factors

Ex. #	*ag*1 (*k** or *k*+1)	*ag*2 (*k*)	*ag*3 (*k*-1)	Comment
1	0.33	0.34	0.33	Centered at *k*
2	0.5	0.5	0.0	Centered at *k*+1/2
3	0.0	1.0	0.0	Explicit
4	1.0	0.0	0.0	Fully Implicit

3 ONE-DIMENSIONAL SUMMARY

Tests in 1-D included looking at stability, sensitivity to the *G* parameter, accuracy and optimum time weights for five domains: constant bathymetry, three cases of parabolic bathymetry and eastcoast bathymetry. Further details on the analysis and procedures are given in a paper by Dresback & Kolar (1999). Important findings from the 1-D work include the following.

- Only one iteration of the corrector step in the new algorithm is necessary to maximize stability.
- At least two-fold gains in the maximum stable time step were seen for most of the domains. For some of the simulations there was a ten-fold increase.
- Maximum increases occurred when nonlinear terms were updated either four at a time or five at a time.
- The GWCE flux times *G* term and the NCM advective terms influence stability the most.
- For variably-spaced grids, stability is influenced by the mesh generating technique.
- *G*-values that produce minimal mass balance errors and errors in the generation of the nonlinear constituents coincide with those that produce the maximum stable time step, viz, G/τ between 2 and 10.
- Stability gains and the optimum set of time weights are somewhat grid and problem dependent. However, we discovered the largest increase in stability usually happened when the time weighting scheme for the nonlinear terms followed the other terms in the two equations. Thus, the GWCE nonlinear terms should be centered at *k* (Example 1 in Table 1) and the NCM nonlinear terms should be centered at *k*+1/2 (Example 2 in Table 1).

4 TWO-DIMENSIONAL DOMAINS

Domains evaluated were the quarter circle harbor and the Bahamas. Six different resolutions (5x5, 10x10, 15x15, 20x20, 25x25 and 30x30) for the quarter circle harbor and a coarse Bahamas discretization make up the experimental grids.

Figure 2 shows the quarter circle harbor with a 10x10 grid resolution; boundary locations are marked. Boundary conditions for the land areas are no flow boundaries, meaning that the normal velocity is set equal to zero, while ocean boundaries have an M_2 tidal forcing, meaning the elevation values vary sinusiodally with a period of 12.42 hours. The Chezy coefficient is set at 0.003 with no eddy viscosity, and the simulation is ramped up from a cold start.

For the Bahamas grid, Figure 3 shows the domain and boundary locations. The ocean boundary has five tidal constituents, M_2, O_1, K_1, S_2, and N_2. Coriolis is set at 5.9×10^{-5} with no eddy visocity and the Chezy coefficient is set at 0.009. The simulation is ramped up from a cold start. Unless noted otherwise, the recommendations from the 1-D experiments were followed.

5 STABILITY EXPERIMENTS

Traditional stability studies, such as Fourier analysis, are valid for linear problems. Here, the nonlinear equations preclude the use of such analytical methods, thus numerical experiments were used to determine stability. For each simulation, the maximum stable time step, to the nearest five seconds, was defined as that which can be used without causing overflow errors before the end of the simulation. Stability changes with the new algorithm were determined from these steps: 1) Each domain was evaluated using the original algorithm to obtain the maximum stable time step; 2) Each domain was evaluated using the new algorithm to obtain the maximum stable time step; 3) Results are used to compute the percent change between the two. It should be noted that since each corrector iteration requires another matrix inversion, only simulations that show more than a $n \times 100\,\%$ change, where *n* is the number of corrector steps, are considered cost-effective. This is a conservative estimate because it assumes the entire load vector is re-evaluated with each iteration, while in reality, only the nonlinear terms need to be updated. Based on 1-D results, only one corrector iteration is performed in all the simulations, therefore only a 100% change is needed for the algorithm to be considered cost-effective. Note that 100% change corresponds to a two-fold increase in the maximum stable time step.

5.1 *Quarter Circle Harbor Domain*

Stability results for this set of experiments are shown in Table 2. Equation 3 gives the formula for the Courant number, *Cr*, which is based on linear wave

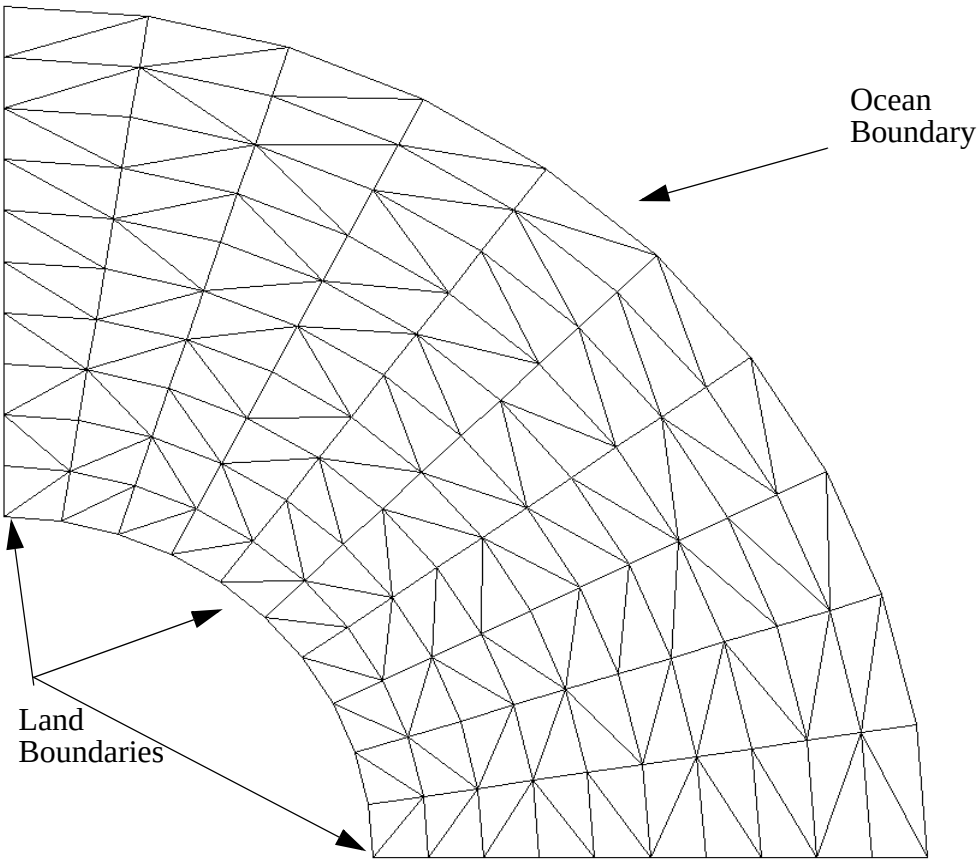

Conditions:

Min. Depth	3.05 m
Max. Depth	19.05 m
inner radius	60,957 m
outer radius	152,393 m
M_2 amplitude	.305 m
# nodes	121
# elements	200

Figure 2. Quarter Circle Harbor Domain (10x10 grid resolution)

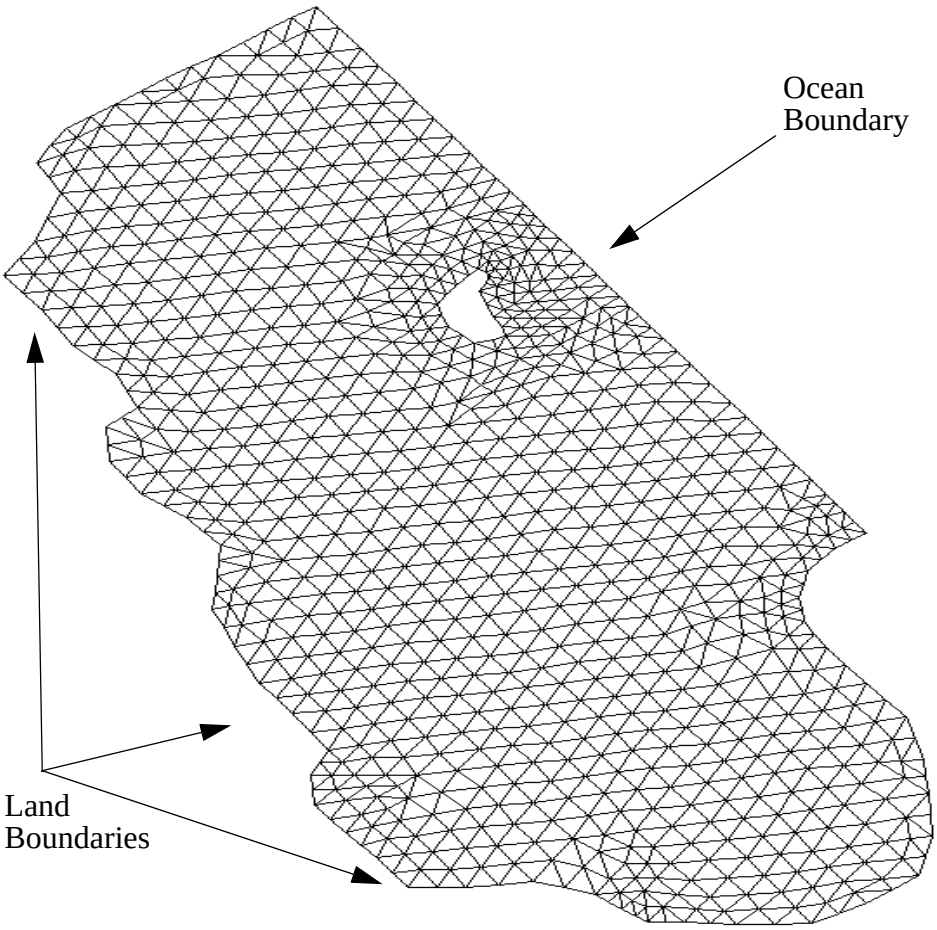

Conditions:

Min. Depth	1.0 m
Max. Depth	9.0 m
M_2 amplitude	0.395 m
O_1 amplitude	0.075 m
K_1 amplitude	0.095 m
S_2 amplitude	0.06 m
N_2 amplitude	0.10 m
# nodes	926
# elements	1696

Figure 3. Bahamas Domain

celerity, $c = \sqrt{gh}$, the minimum node spacing, Δx, and the time step, Δt (held constant for a given simulation).

$$Cr = \frac{c \times \Delta t}{\Delta x} \tag{3}$$

For each quarter circle harbor grid, we computed the Courant number using a minimum bathymetry of three meters (the interior nodes of the domain). *G* was set to 0.001 sec^{-1} for all simulations. Stability results shown here have all six nonlinear terms evaluated implicitly using the time weighting schemes mentioned earlier.

Table 2 Stability Results for Quarter Circle Harbor Bathymetry

Grids	Max. Δt in seconds (Courant #)		Percent Increase
	Original	P-C	
5x5	2210 (0.50)	6970 (1.50)	215%
10x10	1195 (0.5)	4970 (2.07)	316%
15x15	735 (0.45)	4000 (2.47)	444%
20x20	550 (0.45)	3660 (3.00)	565%
25x25	445 (0.45)	3330 (3.40)	648%
30x30	370 (0.45)	3065 (3.75)	728%

Results from these experiments demonstrate that the new algorithm drastically increases the maximum allowable time step. Here the maximum stable time step increases over three-fold (215%) for the coarser grid to over eight-fold (728%) for the finer grid. This demonstrates that all six grids obtain the break-even point of 100%, as was discussed earlier.

We also examined the minimum Courant number for all six of the grids. Theoretically for purely explicit time-marching schemes, the Courant number must be less than one or instabilities will occur in the solution. However in practice, instabilities occur when a Courant number of approximately 0.5 is used with the original time-marching algorithm, even though it was semi-implicit. In Table 2, we see a definite limiting *Cr* value for the semi-implicit algorithm of 0.45 to 0.50. On the other hand, allowable Courant numbers are greater than one in all cases for the predictor-corrector algorithm, ranging from 1.50 to 3.75.

5.2 *Bahamas Domain*

Table 3 shows the stability results for this application. The Courant numbers is obtained using (3), which is based on the variables discussed earlier and a minimum bathymetry of 1.06 meter (near the ocean boundary of the southern part of the domain). *G* was set to 0.005 sec^{-1} for all the simulations. Stability results include all six nonlinear terms evaluated implicitly using the time weighting schemes mentioned earlier.

Table 3 Stability Results for Bahama Bathymetry

Grid	Max. Δt in seconds (Courant #)		Percent Increase
	Original	P-C	
Bahama	280 (0.53)	1150 (2.18)	311%

With this domain, we again see a considerable increase in the maximum allowable time step. The maximum allowable time step increases over four-fold (311%), which is greater than the break-even point of 100%. For the semi-implicit time-marching algorithm, the Courant number follows the trend seen with the quarter circle domain, i.e., a limiting value of 0.5. While with the new time-marching algorithm, we obtain a higher limiting value for the Courant number, equal to 2.18.

5.3 *Summary*

With the implicit time-marching algorithm, we found that the Courant stability constraint is relaxed. With each of these domains, the maximum stable time step increases at least three-fold, and up to eight-fold is possible. For the quarter circle harbor domain, the *Cr* values ranged from 1.5 to 3.75, with the values increasing as the grid was refined. This is a very good trend because the fine grid applications are where we have the most stringent constraints (with the current code). A maximum *Cr* value for the Bahamas domain was determined to be 2.18. Based on these two domains, a good rule of thumb for *Cr* values would be 1.5 to approximately 2.0, with lower values being needed for coarser resolutions. Finally, we caution the user that simulation results deteriorate rapidly as one approaches the maximum stable time step. Therefore, something less than the upper bound (e.g. 90%) should be used in practice.

6 ANALYSIS OF NONLINEAR TERMS

In this section, we evaluate each of the nonlinear terms individually to determine their relative influence. Analyses in 1-D showed that the two most influential terms were the GWCE flux times *G* term and the advective term of the NCM equation. Other nonlinear terms showed importance only in certain situations. For example, the GWCE flux time τ is only important if the τ values are approximately the same magnitude as the *G* values. For any term to be consid-

ered influential, we look for a percent change that is near the break-even point of 100%.

For each of the nonlinear terms, we determined the maximum stable time step when only the nonlinear term under study was "turned on" and all the other nonlinear terms were "turned off". "Turned on" means that the time weighting scheme for that particular nonlinear term follows example 1 or 2 in Table 1, while "turned off" follows example 3 in Table 1. Note that when the terms are "turned off", they return back to the explicit evaluation.

6.1 *Quarter Circle Harbor Domain*

In this domain, a G value of 0.001 sec^{-1} was used for all of the simulations. We found that for all six grid resolutions, the most influential term was the GWCE flux times G term, with increases in the maximum time step greater than the break-even point (160% to 660%). All other terms produced results that did not reach the break-even point of 100%. In fact, their maximum stable time step tends to be nearly the same as that found with the original formulation.

6.2 *Bahamas Domain*

For this domain, a G value of 0.005 sec^{-1} was used for all the simulations. Again, results show the most influential term is the GWCE flux times G term. Increases in the maximum stable time step (230%) are greater than the break-even point. The other nonlinear terms produced results well below the break-even point of 100% and therefore these nonlinear terms are not as influential as the GWCE flux times G term by itself.

6.3 *Summary*

From these results, we can determine the most influential term of all the nonlinear terms is GWCE flux times G. Many of the other terms provide some improvements to the stability, but do not obtain the break-even point. However, one should note that when the other nonlinear terms are updated simultaneously with the GWCE flux times G term, they had a bigger impact on the maximum stable time step than any single individual term. Thus, there must be "synergy" of sorts between terms i.e., stability is enhanced by treating all terms consistently.

7 *G* SENSITIVITY STUDIES

As noted in the previous section, the single most influential nonlinear term is the GWCE flux times G term. This finding was true for all the domains tested so far, 1-D and 2-D. For this study, we wanted to determine the affect of G, the numerical parameter in the GWCE equation, on the maximum stable time step. We note that in previous work by Kolar et al. (1994), a range of G/τ_{max} values (2 to 50) has been shown minimize mass balance errors and errors in the generation of nonlinear constituents. But they also note that as the G/τ_{max} ratio increases above 10, oscillations may start to appear in the solution. Thus, the "optimum" range of G that minimizes mass balance and nonlinear constituents errors is between τ_{max} to $10\tau_{max}$ for the quarter circle harbor and the Bahamas. For nonlinear applications, the closure equation for bottom friction is given by

$$\tau = C_f\sqrt{(u^2 + v^2)}/H, \tag{4}$$

where u, v are the velocity values for the simulation, C_f is the Chezy coefficient, and $H = h + \zeta$ is the total water column depth. Maximum τ occurs in regions with a high velocity field and shallow depth.

Sensitivity analyses were conducted on the two domains, quarter circle harbor and Bahamas. For the new implicit time-marching algorithm, the G parameter ranged between $5x10^{-6}$ to 0.5 sec^{-1} for each of the domains. Simulations used the new predictor-corrector algorithm, with all the GWCE nonlinear terms centered at k and the NCM nonlinear term centered at k+1/2. For each parameter value, the maximum stable time step was obtained, which was then compared to the maximum stable time step from the original algorithm with G held constant at 10^{-3} sec^{-1} for the quarter circle harbor domain and 0.005 sec^{-1} for the Bahamas domain.

7.1 *Quarter Circle Harbor Domain*

Figure 4 shows the results for these sensitivity studies for three grid resolutions, 10x10, 20x20 and 30x30. Using (4), we determined that for this domain τ_{max} is approximately equal to 10^{-4} sec^{-1}, which means the "optimum" range for G is 10^{-3} to 10^{-4} sec^{-1}. For all the grids examined, the greatest percent increase in stability occurs when G ranges between 10^{-3} and 10^{-4} sec^{-1}. For example, for finer resolutions of the grid, we see peaks in the percent increase in stability with G values of 0.0008 sec^{-1} (30x30) and 0.0005 sec^{-1} (20x20). From this information, it is evident that the G values for maximum stability for these grids lie in the range of 10^{-3} to 10^{-4} sec^{-1}, which coincides with the "optimum" range of G from a mass balance and constituent error point-of-view.

7.2 *Bahamas Domain*

Figure 5 shows the results for these sensitivity studies for the Bahamas domain. We determined τ_{max}, using (4), to be approximately 10^{-3} sec^{-1} for this domain, meaning the "optimum" range for G is 10^{-2} to 10^{-3} sec^{-1}. Greatest percent increase in stability occurs when the G parameter ranges from 10^{-2} to 10^{-3} sec^{-1}

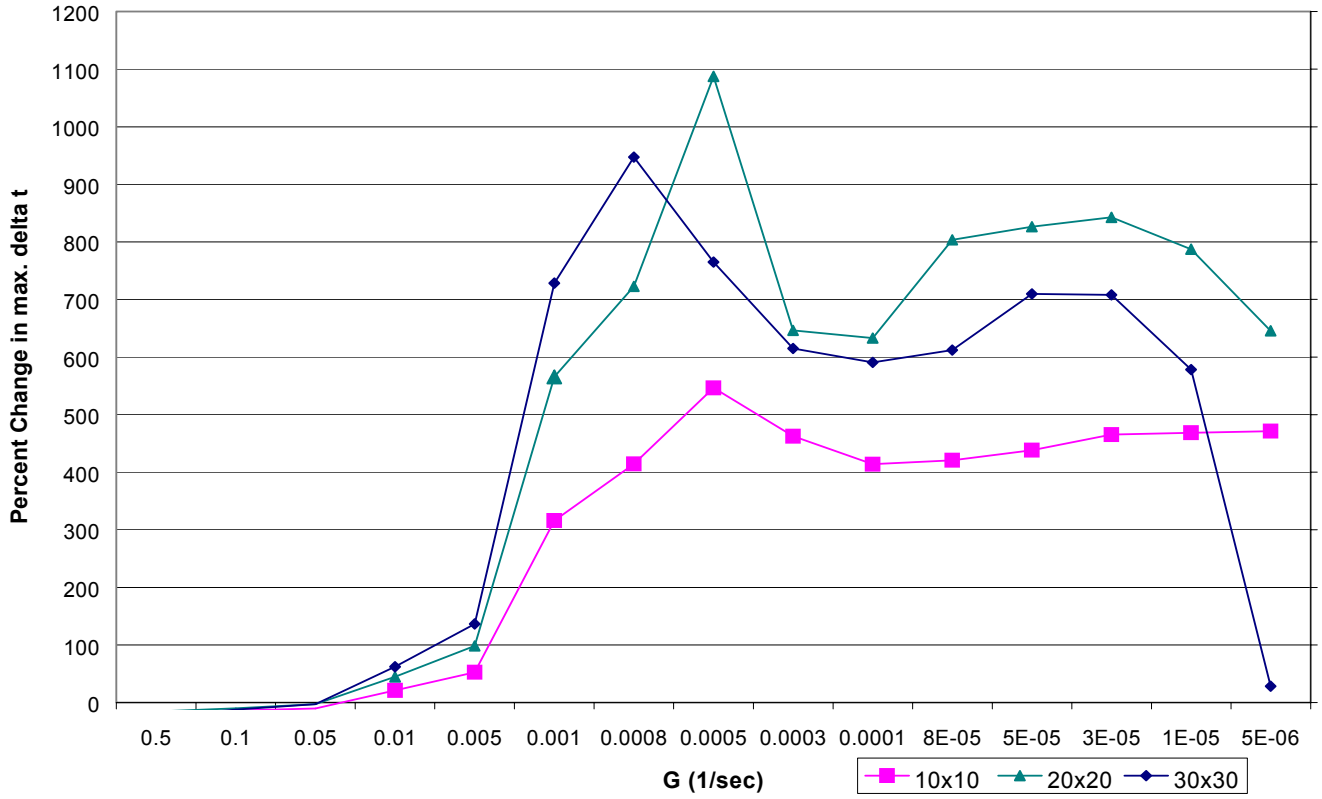

Figure 4. *G* sensitivity graph for three resolutions of the quarter circle harbor domain

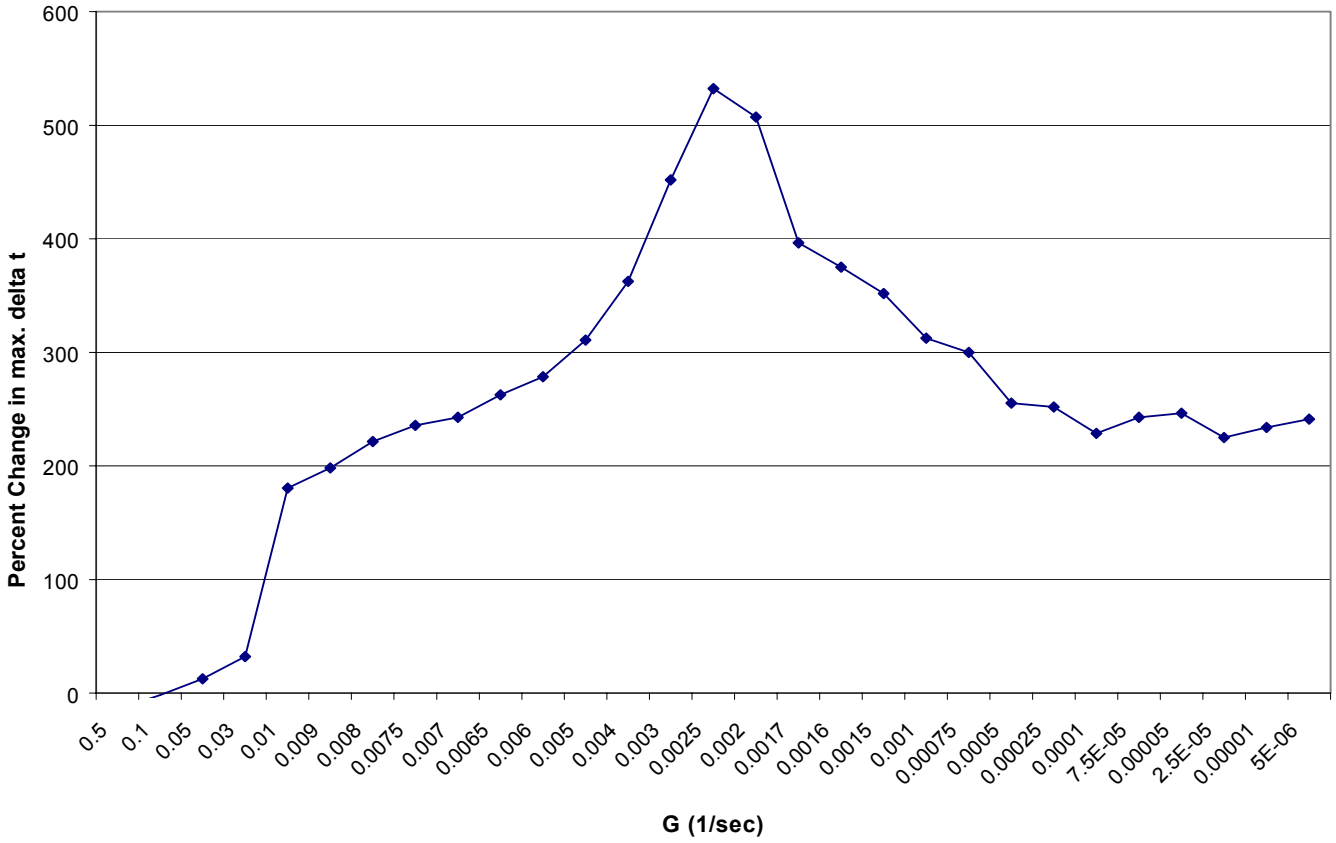

Figure 5. *G* sensitivity graph for the Bahamas domain

with the peak occurring at a G parameter value of 0.0025 sec^{-1}. From this information, it is evident that the G values for maximum stability of these grids lie within the range of 10^{-2} to 10^{-3} sec^{-1}, which coincides with the "optimum" range of G from a mass balance and constituents error point-of-view.

7.3 *Summary*

Comparing these results to the previous work by Kolar et al. (1994), we can see that the "optimum" range of G for these two domains overlaps with the range of G values that produce the greatest increase in stability. Thus, if we keep G/τ_{max} values between 1 and 10, we will be able to see both an increase in stability and a decrease in mass balance errors and errors in the generation of nonlinear constituents.

8 CONCLUSIONS AND FUTURE WORK

Primary objectives for this study were to examine the use of a predictor-corrector time-marching algorithm for two-dimensional simulations and quantify its affect on stability. In general, results show a dramatic increase in the maximum stable time step for the two domains examined. Some significant conclusions that we can draw from this study are listed below.

- When evaluating the nonlinear terms together with the new algorithm, there is always 100% gain in the maximum stable time step. For one of the grid resolutions, we saw over a eight-fold increase.
- Stability results show maximum increases when the nonlinear terms were evaluated all together with the appropriate time weighting scheme.
- Analysis of individual terms show that the GWCE flux times G term has the greatest influence on stability.
- From the G sensitivity study, it is evident that the G values that produce minimal mass balance errors and errors in the generation of the nonlinear constituents coincide with those that produce the maximum stable time step (G/τ_{max}=1 to 10).
- Results show that the Courant number constraint can be increased from 0.5 for the semi-implicit time-marching algorithm to approximately 1.5 to 2.0 for the two domains examined with the implicit time-marching algorithm.

It is apparent from these results that the new implicit time-marching algorithm significantly enhances the ability of ADCIRC to perform fast, reliable simulations. Future work includes looking at larger, more complicated domains, such as the Gulf of Mexico, Western North Atlantic, and also some Pacific grids. We will also look at the accuracy effects of the new algorithm that parallels our 1-D assessment.

9 ACKNOWLEDGEMENTS

Financial support for this research was provided in part by the National Science Foundation under the contract ACI-9623592. We would also like to thank Casey Dietrich for his help in conducting the numerical experiments.

10 REFERENCES

Blain, C.A. 1994. *The influence of domain size and grid structure of a hurricane storm surge model.* Ph.D Dissertation, Univ. of Notre Dame, IN.

Dresback, K.M. & R.L. Kolar. 1999. An implicit time-marching algorithm for shallow water models based on the generalized wave continuity equation. *International Journal for Numerical Methods in Fluids*, in review.

Gray, W.G. & D.R. Lynch. 1977. Time-stepping schemes for finite element tidal model computations. *Advances in Water Resources* 2(1): 83-95.

Kinnmark, I.P.E. & W.G. Gray. 1984. An implicit wave equation model for the shallow water equations. *Advances in Water Resources*. 7:168-171.

Kinnmark, I.P.E. 1986. *The shallow water wave equations: formulations, analysis, and application (Lecture notes in engineering, Vol. 15)*, Springer-Verlag, Berlin.

Kolar, R.L., J.P. Looper, W.G. Gray & J.J. Westerink. 1998. An improved time marching algorithm for GWC shallow water models. In Burganos et al. (ed.), *CMWR XII Volume 2: Computational Methods in Surface Flow and Transport Problems*: 379-385.

Kolar, R.L., W.G. Gray, J.J. Westerink & R.A. Luettich 1994. Shallow water modeling in spherical coordinates: equation formulation, numerical implementation and application. *Journal of Hydraulic Research*. 32(1):3-24.

Kolar, R.L., J.J. Westerink, M.E. Cantekin & C.A. Blain 1994. Aspects of nonlinear simulations using shallow-water models based on the wave continuity equation. *Computers Fluids* 23(3): 523-538.

Lee, J.K. & D.C. Froehlich 1986. *Review of literature on the finite-element solution of the equations of two-dimensional surface-water flow in the horizontal plane*. U.S. Geological Survey Circular 1009. USDOI, Denver, CO.

Luettich, R.A., J.J. Westerink & N.W. Scheffner 1991. *ADCIRC: an advanced three-dimensional circulation model for shelves, coasts and estuaries; report 1: theory and methodology of ADCIRC-2DDI and ADCIRC-3DL*, Technical Report DRP-92-6, Dept. of the Army, USACE. Washington, D.C.

Lynch, D.R. & W.G. Gray 1979. A wave equation model for finite element tidal computations. *Computers and Fluids*. 7(3):207-228.

Westerink, J.J., R.A. Luettich, C.A. Blain & N.W. Scheffner 1992. *ADCIRC: an advanced three-dimensional circulation model for shelves, coasts and estuaries; report 2: users manual for ADCIRC-2DDI*, Dept. of the Army, USACE. Washington, D.C.